Indirect co-cultivation of HepG2 with differentiated THP-1 cells induces AHR signalling and release of pro-inflammatory cytokines

Florian Padberg[a,b,*], Henrik Hering[a], Andreas Luch[a,b], Sebastian Zellmer[a]

[a] *German Federal Institute for Risk Assessment (BfR), Department of Chemical and Product Safety, Max-Dohrn Strasse 8-10, 10589 Berlin, Germany*
[b] *Department of Biology, Chemistry, Pharmacy, Institute of Pharmacy, Freie Universität Berlin, Berlin, Germany*

ABSTRACT

HepG2 and THP-1 cells, the latter differentiated by phorbol 12-myristate 13-acetate (PMA), were co-cultured and characterized for typical liver-specific functions, such as xenobiotic detoxification, lipid and cholesterol metabolism. Furthermore, liver injury-associated pathways, such as inflammation, were studied. In general, the co-cultivation of these cells produced a pro-inflammatory system, as indicated by increased levels of cytokines (IL-8, TGF-α, IL-6, GM-CSF, G-CSF, TGF-β, and hFGF) in the respective supernatant. Increased expression levels of target genes of the aryl hydrocarbon receptor (AHR), *e.g.*, *CYP1A1*, *CYP1A2* and *CYP1B1*, were detected, accompanied by the increased enzyme activity of CYP1A1. Moreover, transcriptome analyses indicated a significant upregulation of cholesterol biosynthesis, which could be reduced to baseline levels by lovastatin. In contrast, total *de novo* lipid synthesis was reduced in co-cultured HepG2 cells. Key events of the adverse outcome pathway (AOP) for fibrosis were activated by the co-cultivation, however, no increase in the concentration of extracellular collagen was detected. This indicates, that AOP should be used with care. In summary, the indirect co-culture of HepG2/THP-1 cells results in an increased release of pro-inflammatory cytokines, an activation of the AHR pathway and an increased enzymatic CYP1A activity.

1. Introduction

The liver is the main organ of intermediary metabolism. When taken up orally, nutrients, noxious and/or pharmacologically active compounds reach the liver through the portal vein. Consequently, appropriate *in vitro* liver models are widely discussed and developed for toxicological and pharmacological studies (Zeilinger et al., 2016; Soldatow et al., 2013; Toyoda et al., 2017; Zhou et al., 2019). Primary human liver cells are thus far the "gold standard" for these *in vitro* investigations (Zeilinger et al., 2016; Soldatow et al., 2013). However, one should be aware of the short comings of this "gold standard", for instance, large inter-individual differences, reduction in functionality within days (Soldatow et al., 2013) and induction of signalling pathways and changes in enzyme activity due to disease-related patient treatment. On the other hand, hepatic cell lines (*e.g.*, HepG2, Huh7) also have limitations, since the metabolic enzyme activity of these cells is often much lower or absent than that of primary cell cultures (Hewitt and Hewitt, 2004; Lin et al., 2012). However, availability is almost unlimited, since these cells can be easily expanded in the laboratory.

Differences between primary human hepatocytes and HepG2 cells in the response to pharmacologically active substances were investigated recently (Albrecht et al., 2019). Primary hepatocytes were more suitable for the detection of toxic effects, compared to HepG2 cells. In addition, it was shown that the read out was of crucial importance. The authors concluded that HepG2 cells represent a suitable screening tool to study most of these substances (Albrecht et al., 2019). Besides the single cultivation of HepG2 cells, co-culturing of HepG2 cells (*e.g.* with THP-1 cells) could also lead to more sensitive cell culture model. However, much more complex 3D co-cultures have generated promising pro-fibrotic hepatic *in vitro* systems (Prestigiacomo et al., 2017). In this system, essential interactions between hepatocytes, Kupffer cells and stellate cells (by HepaRG, THP-1, hTERT-HSC) were successfully simulated *in vitro*. This study showed that co-cultivation systems could have a higher validity compared to single cultures and that THP-1 cells can be a possible surrogate for human Kupffer cells. (Prestigiacomo et al., 2017).THP-1 cells, differentiated by phorbol 12-myristate 13-acetate (PMA), convert into a macrophage-like phenotype (Schwende et al., 1996). Wewering and co-workers (Wewering et al., 2017a)

---

established an indirect co-cultivation system with HepG2 and PMA-differentiated THP-1 cells. This co-cultivation resulted in a pro-inflammatory system, as indicated by the secretion of C–X–C-motif ligand 8 (CXCL8 or IL-8), granulocyte macrophage colony-stimulating factor (GM-CSF) and macrophage migration inhibitory factor. Granitzny and co-workers (Granitzny et al., 2017) investigated the suitability of this co-cultivation system for the identification of drugs that induce liver injury (DILI). Positive reference substances for DILI like troglitazone, trovafloxacin, diclofenac and ketoconazole as well as negative reference substances like rosiglitazone, levofloxacin, acetylsalicylic acid, fluconazole were correctly identified and proved the functionality of the system. In addition, tumour necrosis factor α (TNF-α) was identified as a prognostic factor for DILI development *in vitro* (Granitzny et al., 2017). These findings support the hypothesis that pro-inflammatory conditions might lower the hepatotoxic thresholds of xenobiotics or drugs and can lead to DILI (Roth et al., 2003).

The main focus of the present paper are changes at the cellular level that were induced by the indirect co-cultivation of HepG2 and PMA-differentiated THP-1 cells. Therefore, gene expression profiles were determined by transcriptome analyses. The predictions were then validated by measuring cytokine secretion, CYP enzyme expression and specific enzyme activities, collagen accumulation and changes in the amount of total lipids. Finally, crucial hepatic pathways that were changed due to the co-cultivation conditions were identified, which allows a deeper understanding of the co-cultivation system.

2. Methods

All methods were carried out according to the manufacturer's protocol. Only the modifications are given below.

2.1. Chemicals and antibodies

All chemicals were purchased from Sigma-Aldrich (Taufkirchen, Germany) unless stated otherwise. In general, Dulbecco's phosphate-buffered saline (DPBS, PAN-Biotech, Aidenbach, Germany) was used. A list of the antibodies used is provided in supplementary table S1.

2.2. Cell culture

All single use consumables were purchased from TPP (Trasadingen, Switzerland). Cell lines were purchased from DSMZ (Braunschweig, Germany). HepG2 cells were grown in RPMI 1640 (PAN-Biotech, Aidenbach, Germany) contained 10% (v/v) FCS, 100 U/ml penicillin, 100 mg/ml streptomycin, 2 mM L-glutamine at 37 °C and 5% CO_2 as described previously. THP-1 cells were grown in RPMI 1640 (PAN-Biotech, Aidenbach, Germany) contained 10% (v/v) FCS, 100 U/ml penicillin, 100 mg/ml streptomycin, 2 mM L-glutamine, 1 mM sodium pyruvate, 10 mM Hepes and the co-culture were performed using Falcon® cell culture inserts (VWR, Darmstadt, Germany) according to Wewering and co-workers (Wewering et al., 2017a). HepG2 cells were seeded at a density of 1.3×10^5 cells per cm^2. THP-1 cells were seeded at a density of 0.65×10^5 cells per cm^2 and differentiated using 100 nM phorbol-12-myristat-13-acetat (PMA) for 24 h. Immediately after differentiation the co-cultivation with the HepG2 cells was started. Previously it has been shown that PMA in the concentration range of 8–200 nM can be used for a successful differentiation and adherence of the cells to the culture vessel within 24 h (Lund et al., 2016). However, during a subsequent PMA free cultivation phase the adherence decreased with a decreasing PMA concentration. THP-1 cells, that were differentiated with 100 nM PMA showed the highest adherence 24 h after cultivation in the absence of PMA. Secondly, the concentration of PMA as well as incubation and resting phase seems to affect the toxicity of drugs. Granitzny and co-workers (Granitzny et al., 2017) studied the effect of ketoconazole on THP-1 cells, differentiated for 72 h in the presence of 50 nM PMA, followed by a resting phase in PMA-free

growth medium for another 24 h. In co-culture, ketoconazole had a much higher toxicity to THP-1 cells, compared to the HepG2 cells (Granitzny et al., 2017). In contrast, the differentiation with 100 nM PMA for 24 h without a resting phase decreased the toxicity of ketoconazole (Wewering et al., 2017a). In order to warrant a high adherence of the THP-1 cells and a similar toxicity of drugs to THP-1 cells and HepG2 cells, 100 nM PMA was used for differentiation.

In Fig. 1 the set-up of a co-cultivation can be seen. In order to further investigate the differentiation protocol used, the basic property of phagocytosis of PMA differentiated THP-1 cells (Kurynina et al., 2018) was confirmed (Fig. 1B). The THP-1 cells were capable of active phagocytosis from the beginning of co-cultivation to the end. Therefore, all cultures were incubated for 24 h and culture medium with 0.1% DMSO was used as control.

2.3. Cell viability testing

The MTT Assay was performed according to Mosmann (Mosmann, 1983). All values were corrected for the solvent control DMSO.

2.4. RNA isolation

RNA was isolated using the NucleoSpin® RNA Kit (Machery-Nagel, Düren, Germany).

2.5. Microarray analyses

All samples (RNA integrity number (RIN) > 8.5) were analysed using a Human Clariom™ S Assay (Applied Biosystems, Foster City, CA, USA). Microarray data have been deposited in the Gene Expression Omnibus (GEO) database, www.ncbi.nlm.nih.gov/geo (accession no. GSE140141). To analyse microarray data, the exclusion criterion of $p \leq 0.05$ was used. Detailed information is provided in the supplementary material.

2.6. Cytokines

Cytokines in the supernatant were measured using the Cytokine LEGENDplex™ including Anti-Virus Response Panel (IL-8, IL-6, human fibroblast growth factor (hFGF)), Cytokine Panel 2 (interleukin 1α (IL-1α)) and Growth Factor Panel (TGF-α, GM-CSF, granulocyte colony-stimulating factor (G-CSF)) (Biolegend, San Diego, CA, USA). The results were analysed using LEGENDplex™ 8.0 software (Biolegend, San Diego, CA, USA). TGF-β was quantified using the BD™ Cytometric Bead Array (CBA) with the Human TGF-β1 Single Plex Flex Set (BD Biosciences, Heidelberg, Germany) and analysed with FCAP Array v1.0.1 software (BD Biosciences, Heidelberg, Germany).

2.7. PCR analyses

Reverse transcription was performed with the High-Capacity cDNA Reverse Transcription Kit (Applied Biosystems, Foster City, CA, USA). Quantitative PCR (qPCR) was performed with a 7500 Fast Real-Time PCR Instrument using Fast SYBR Green Master Mix (Applied Biosystems, Foster City, CA, USA). The primer sequences are listed in table S2. The ΔΔCT-value was calculated according to Livak and Schmittgen (Livak and Schmittgen, 2001) and normalized to the expression of hypoxanthine-guanine phosphoribosyl transferase (HPRT) and to the corresponding control sample. Positive controls were generated by the treatment with 10 nM 2,3,7,8-tetrachlorodibenzo-*p*-dioxin (TCDD) (LGC Standards, Wesel, Germany) or 1 μM lovastatin before RNA isolation.

2.8. Western blots

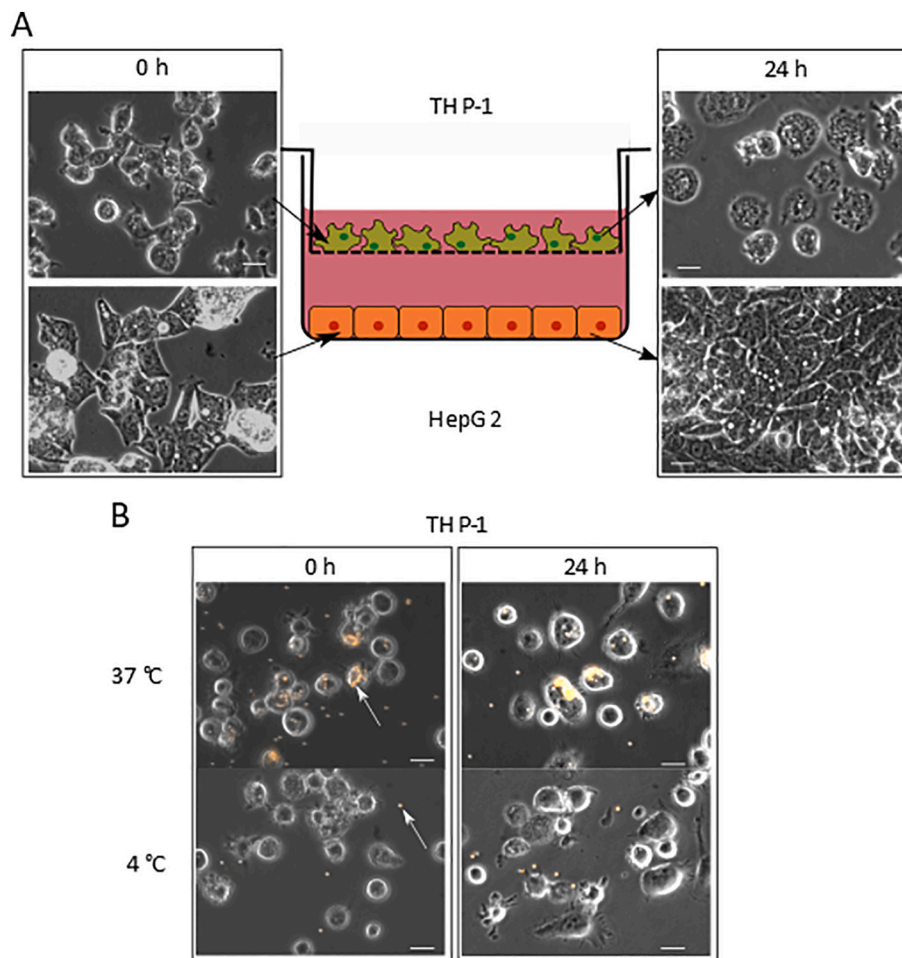Cells were lysed at 4 °C in RIPA buffer (50 mM Tris/HCl (pH 7.4),

Fig. 1. Set-up of the co-cultivation and phagocytic capacity of THP-1 cells. THP-1 cells were differentiated using 100 nM phorbol-12 myristat-13 acetat (PMA) for 24 h and the co-cultivation with HepG2 starts without a resting phase. (A) Shown are set-up und photomicrographic images at the beginning ($t = 0$) and the end ($t = 24$ h) of the co-cultivation. (B) Phagocytosis is a characteristic of PMA differentiated THP-1 cells. The internalization of latex beads (2 μm, 5 μl/ml culture medium) after 2 h incubation is temperature dependent (4 °C or 37 °C). The white arrow indicates exemplarily the latex beads. The scale bar denotes 20 μm.

159 mM NaCl, 1 mM EDTA, 1% Igepal®, 0.25% sodium deoxycholate) supplemented with a protease inhibitor cocktail (Merck, Darmstadt, Germany). Protein concentrations were determined with the Pierce™ BCA Protein Assay Kit (Thermo Scientific, Waltham, MA, USA), and equal amounts of protein were applied to SDS-PAGE and transferred onto nitrocellulose membranes. After binding of primary antibodies (24 h at 4 °C), the secondary antibody (horseradish peroxidase labelled) was added, and visualized with Pierce ECL Substrate (Thermo Fisher Scientific, Waltham, MA, USA) using a ChemiDoc XRS (Bio-Rad, Munich, Germany).

2.9. CYP1A1 activation

CYP1A1 activation was measured using the P450-Glo™ CYP1A1 Assay System (Promega Corporation, Madison, WI, USA).

2.10. Cholesterol measurements

The cholesterol concentration was quantified using the Amplex™ Red Cholesterol Assay Kit (Thermo Fisher Scientific, Waltham, MA, USA).

2.11. Lipid staining

The cellular layer was fixed with Roti®-Histofix 4% (Roth, Karlsruhe, Germany) for 10 min, and cells were permeabilized with 0.2% TRITON™X-100 for 10 min. Lipids were stained using a freshly prepared 6 mM Sudan Red 7 B solution in 60% 2-propanol for 10 min. After carefully removing excess staining solution, nuclear staining was performed with 1 μg/ml Hoechst3342. Images were repeatedly taken using an Olympus BX51 microscope (U Plan FLN 20×/0.50) connected to a ColorView III camera (Olympus, Hamburg, Germany). Finally, the number of nuclei and the areas of stained droplets were calculated using CellProfiler® 3.1.5 software (Carpenter et al., 2006) An example of the evaluation and its calculation is given in fig. S1.

2.12. ATP measurements

The ATP concentration was determined using a Bioluminescence Assay Kit HS II (Roche, Basel, Switzerland).

2.13. Collagen staining

The Sirius Red/Fast green collagen staining kit (AMS Biotechnology, Abingdon, UK) was used.

2.14. Statistics

Detailed information on the exploratory grouping analysis is provided in the supplementary section. All data shown contain at least three independent biological replicates. Means, standard deviations and ANOVA *p*-values followed by Bonferroni correction were calculated

with GraphPad Prism 6 (Statcon, Witzenhausen, Germany). Analysed gene lists were selected due to the pathway relevance and the significance ($p < 0.05$) using Ingenuity® Pathway Analysis (Qiagen, Aarhus, Denmark). The Z-score and the hierarchical clustering were calculated with Perseus Software (Tyanova et al., 2016). Three-dimensional figures were generated using Plotly (https://plot.ly) (Plotly Technologies Inc, 2015).

3. Results

3.1. Toxicity of selected substances on 100 nM PMA diffentiated THP-1 cells

The toxicity of drugs, used in co-cultivation experiments should have similar half effective concentrations for all cell lines. PMA differentiated THP-1 cells are very sensitive against drugs (Granitzny et al., 2017). Therefore, in a first step, we tested the effect of three different drugs on the cell viability of PMA differentiated THP-1 cells, after single and co-culture. The selected PMA concentration was 100 nM (c.f. 2.2).

The loss of cell viability induced by primaquine, flutamide and amiodarone (Fig. 2) was almost lower or equal (Fig. 2) for co-cultivated THP 1 cells compare to the corresponding single cultivation. Therefore, THP-1 differentiation with 100 nM PMA for 24 h without a resting phase was chosen for all experiments, in order to obtain high adherence and low loss of viability of the THP-1 cells.

3.2. Exploratory grouping analysis highlights differences between single- and co-cultivated HepG2 cells

Outlier and batch effects can occur if there are any differences in batch-to-batch cultivation conditions or in the handling and preparation of samples. These outliers can be identified, for example, by exploratory grouping analysis (Bro and Smilde, 2014). We compared the cultivation conditions (single- and co-cultivation) of HepG2 cells and PMA-differentiated THP-1 cells (Fig. 3). The distances of the individual samples in terms of expression profiles indicate that the variation in the data is mainly affected by culture conditions (single- *vs.* co-cultivation) and the kind of cell type (HepG2 or THP-1), but not by batch-to-batch variations between individual samples. Therefore, the presence of

outliers and a batch-to-batch variation was excluded and all samples were included in the subsequent analyses.

3.3. Genes associated with liver inflammation are upregulated

The analysis of the transcriptomes identified differentially expressed cytokines and cytokine receptors. A total of 73.9% of the significantly upregulated genes ($p < 0.05$) were associated with liver inflammation (Fig. 4A). Based on these microarray data, we quantified a selection of secreted cytokines in the cell culture supernatants (Fig. 4B). To identify the cell type responsible for the secretion (HepG2 or THP-1), we also quantified cytokine concentrations in pure THP-1 and HepG2 (single cell) cultures. Among the set of cytokines investigated, hFGF, TGF-α, and G-CSF were only detectable under co-cultivation conditions (Fig. 4B), whereas HepG2 cells alone also secreted GM-CSF and IL-6. However, the levels of these two biomarkers were still further and significantly ($p < 0.01$) upregulated under the condition of co-cultivation with THP-1 cells. Conversely, PMA-differentiated THP-1 cells alone secreted IL-8 to a much higher extent than did HepG2 cells alone. IL-8 levels under co-cultivation conditions were again in the same range as observed for THP-1 cells in the absence of HepG2 cells. In contrast, TGF-β concentrations in the supernatant were 2-fold higher (non-significantly) under co-cultivation than in individual cell cultures but represented approximately the sum of levels that were measured in the latter. Interestingly, the cytokine IL-1α was only detectable when THP-1 cells were cultured alone but absent in HepG2 cell cultures or co-cultures of THP-1 and HepG2 cells.

In conclusion, the secretion differed between individually cultivated cells and the co-cultivation of HepG2 with differentiated THP-1 cells (Fig. 4).

3.4. Pro-inflammatory conditions in co-culture activate the AHR signalling pathway

Next, we were interested, whether xenobiotic metabolism might be affected under co-culture conditions. Therefore, genes representing phase I and phase II xenobiotic metabolism whose expression levels were found to be significantly elevated were selected from the microarray data (Fig. 5A). Using Ingenuity® Pathway Analysis (IPA®) software, we concluded that most (70.0%) of these genes were
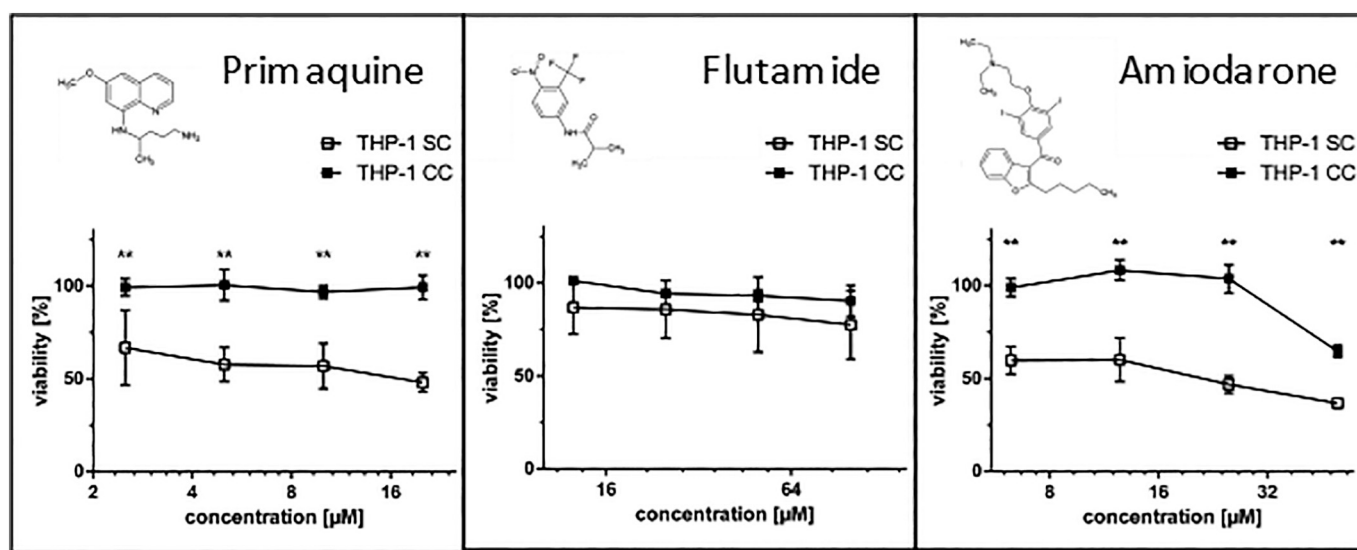

Fig. 2. Dose dependent loss of cell viability on co- and single-cultivated THP-1 cells. THP-1 cells were exposed to increasing concentration of primaquine, flutamide, or amiodarone for 24 h in co- (CC) or single-(SC) cultivation condition. Viability was determined using a MTT assay. All values were corrected to % of the corresponding DMSO solvent controls. $n = 3$, **$p < 0.01$.
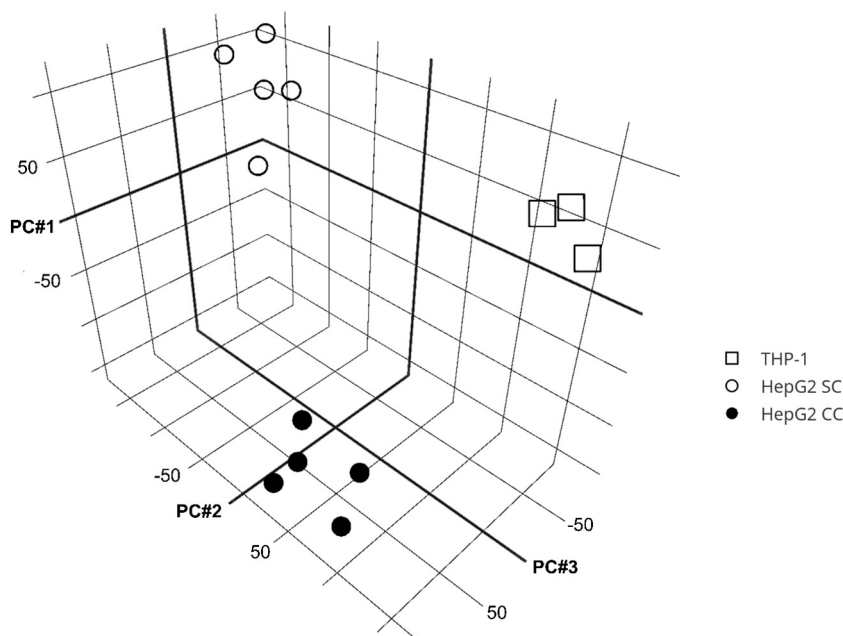
Fig. 3. Exploratory grouping analysis shows that the cultivation conditions affect gene expression profiles to a larger extent than the factor of sample-to-sample variability within the same group. HepG2 cells were cultivated with PMA-differentiated THP-1 cells in co-culture (●, HepG2 CC, $n = 5$) and compared to single cultivated HepG2 (○, HepG2 SC, $n = 5$) or PMA-differentiated THP-1 (single cell) cultures (□, THP-1, $n = 3$) for 24 h.
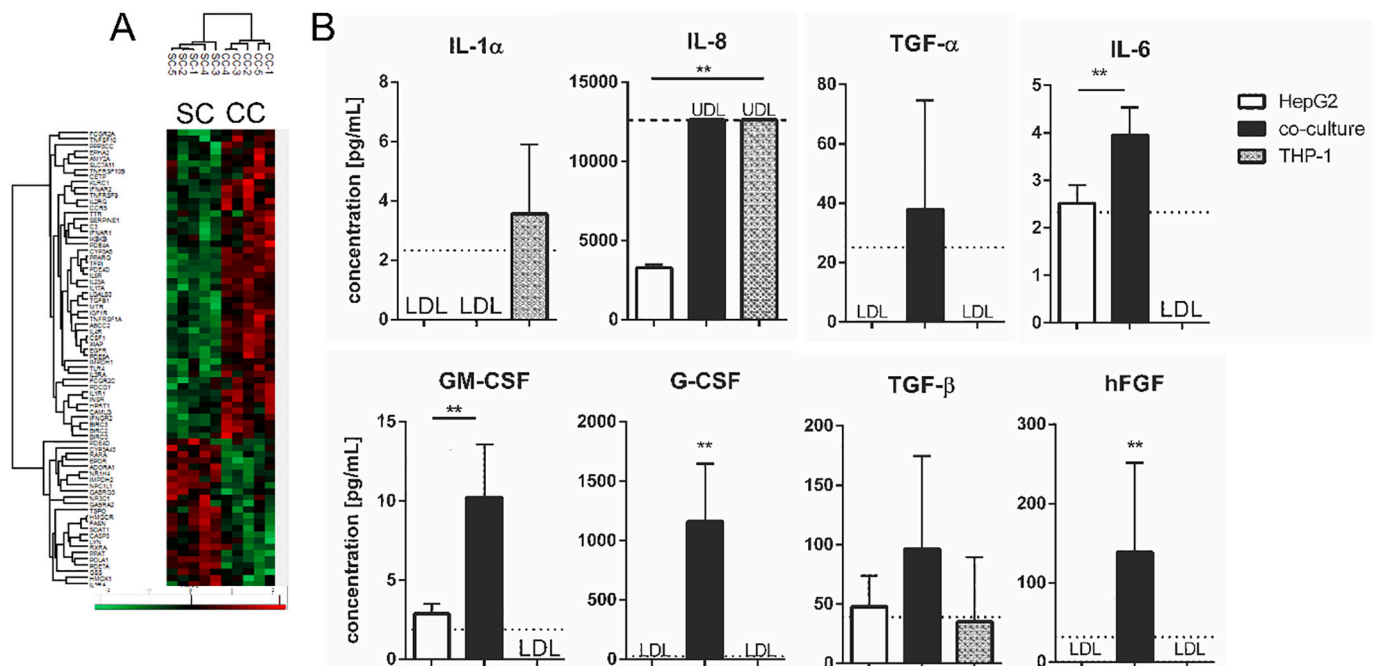

Fig. 4. Inflammation is induced in the co-culture of HepG2 and differentiated THP-1 cells. (A) Heat map of HepG2 cells in single culture (SC) or co-culture (CC) with PMA-differentiated THP-1 cells after 24 h ($n = 5$). Gene symbols and the Z-score of significantly (exclusion $p > 0.05$) up- or downregulated genes based on the IPA gene list are shown. An enlarged heat map is shown in the supplementary material (S2). (B) Secretion of TNF-α, IL-8, TGF-α, IL-6, GM-CSF, G-CSF, TGF-β and hFGF in the supernatant of individually cultured and co-cultivated cells after 24 h ($n = 6$). The means and standard deviations (SD) are shown with the upper (UDL) (− −) and the lower detection limits (LDL) of the assay (···). **$p < 0.01$.

downregulated (Fig. 5A). In addition, the IPA® analysis indicated the activation of the AHR in co-culture. Immunoblot assays confirmed an increase in the amount of AHR protein in HepG2 cells after co-cultivation and a comparable amount of aryl hydrocarbon receptor nuclear translocator (ARNT) (Fig. 5B). As a result, known AHR target genes were transcriptionally upregulated in co-cultivated HepG2 cells compared to single-cultivated HepG2 cells (Fig. 5C): 74-fold for *CYP1A1*, 48-fold for *CYP1A2* and 4-fold for *CYP1B1*.

Next, we studied, whether a classical inductor of AHR, 2,3,7,8-tetrachlorodibenzo-*p*-dioxin (TCDD), is able to further induce the expression of AHR target genes in co-culture. Therefore, we treated single- and co-cultivated cells with the AHR activator TCDD. Compared to treated single-cultivated HepG2 cells, the co-cultivated HepG2 cells showed clearly upregulated *CYP1A2* and *CYP1B1* gene expression, only (Fig. 5D). The additional induction of CYP1A1 by TCDD was only minor. Finally, we were interested, whether the increased gene and protein expression resulted in increased enzyme activity of the target gene. The enzyme activity of CYP1A1 was significantly higher ($p < 0.01$) in co-cultivated HepG2 cells than in individually cultivated HepG2 cells (Fig. 5E), indicating that the AHR receptor pathway was
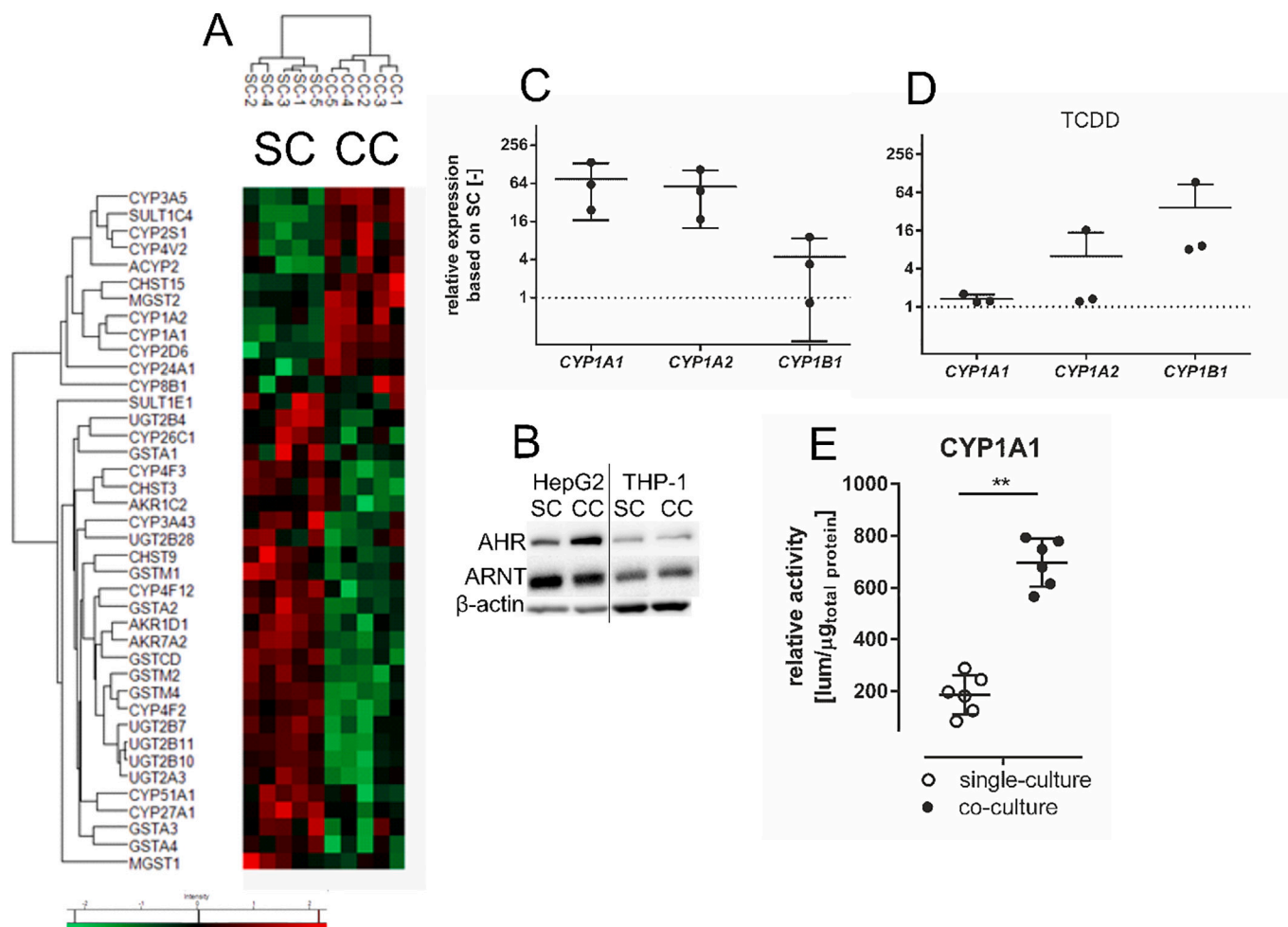
Fig. 5. Effects of co-cultivation on xenobiotic metabolism. (A) HepG2 cells were cultivated in single culture (SC) or co-culture (CC) for 24 h ($n = 5$). The gene symbols and the Z-score of significantly and differentially expressed genes are shown. (B) Co-cultivation increased the amounts of AHR and ARNT. One representative blot of three biological replicates is shown. (C) Co-culture of HepG2 cells resulted in the increased expression of CYP1A1 and CYP1A2 gens, compared to single-cultivated cells. (D) Addition of 10 nM TCDD in CC systems resulted in no further induction of cytochrome P450 1A1 (*CYP1A1*), but an additional induction of cytochrome P450 1A2 (*CYP1A2*), and cytochrome P450 1B1 (*CYP1B1*) expression ($n = 3$). (E) Compared to individually cultivated cells, HepG2 cells in co-culture showed increased cytochrome P450 1A1 (CYP1A1) enzyme activity ($n = 6$). **$p < 0.01$.

not only activated but also resulted in higher amounts of functional enzyme.

This result implies that compared to the individual cultivation of HepG2 cells, the co-cultivation of HepG2 cells with differentiated THP-1 cells results in the activation of AHR target genes and an increased CYP1A1 enzyme activity.

3.5. Cholesterol biosynthesis is enhanced in co-culture

The liver is the main organ of cholesterol synthesis. The microarray data revealed that all genes in the cholesterol biosynthesis pathway were significantly ($p < 0.05$) downregulated under co-cultivation compared to individual cultivation (Fig. 6A). In contrast, the cellular cholesterol concentration was significantly increased in co-cultivated HepG2 cells after 24 h relative to the individually cultivated cells (Fig. 6B). Thus, we studied these contradictory results in more detail. HepG2 cells were treated with the HMG-CoA reductase inhibitor lovastatin, and the expression of a master regulator of cholesterol synthesis, sterol regulatory element binding transcription factor 1 (*SREBF1*) (Shimano et al., 1996), was determined (Fig. 6C). As expected, lovastatin treatment induced the significant upregulation (2-fold) of the transcription factor *SREBF1* in single culture. In co-culture, however, a 1.5-fold downregulation was detected (Fig. 6C). This

treatment-dependent regulation indicated the presence of a negative feedback mechanism in co-culture. For clarification, we determined the cellular cholesterol concentration in single- and co-cultivated HepG2 cells after lovastatin treatment. In single-cultivated cells, the amount of cholesterol decreased relative to the level in co-cultivated cells (Fig. 6B). To further evaluate the effect of lovastatin, we compared individually cultivated and co-cultivated cells at different time points. In individually cultivated HepG2 cells, the effect of lovastatin occurred after 48 h (Fig. 6D). However, in co-cultivated cells, a significant ($p < 0.05$) reduction in the cellular cholesterol concentration occurred after 24 h and remained constant for 48 h (Fig. 6D), indicating that lovastatin affected the lipid metabolism in co-cultivated cells responded faster than in individually cultivated cells.

In summary, we have shown that cholesterol biosynthesis is increased in co-cultivated HepG2 cells, despite reduced *SREBF1* expression. The cholesterol-lowering effect of lovastatin occurred earlier in co-culture than in individual culture.

3.6. Total lipid synthesis is decreased in co-culture

Next, we were interested, whether the total lipid amount and the related metabolism were affected during co-cultivation. Transcriptional analysis showed that 65% of the significantly ($p < 0.05$) regulated
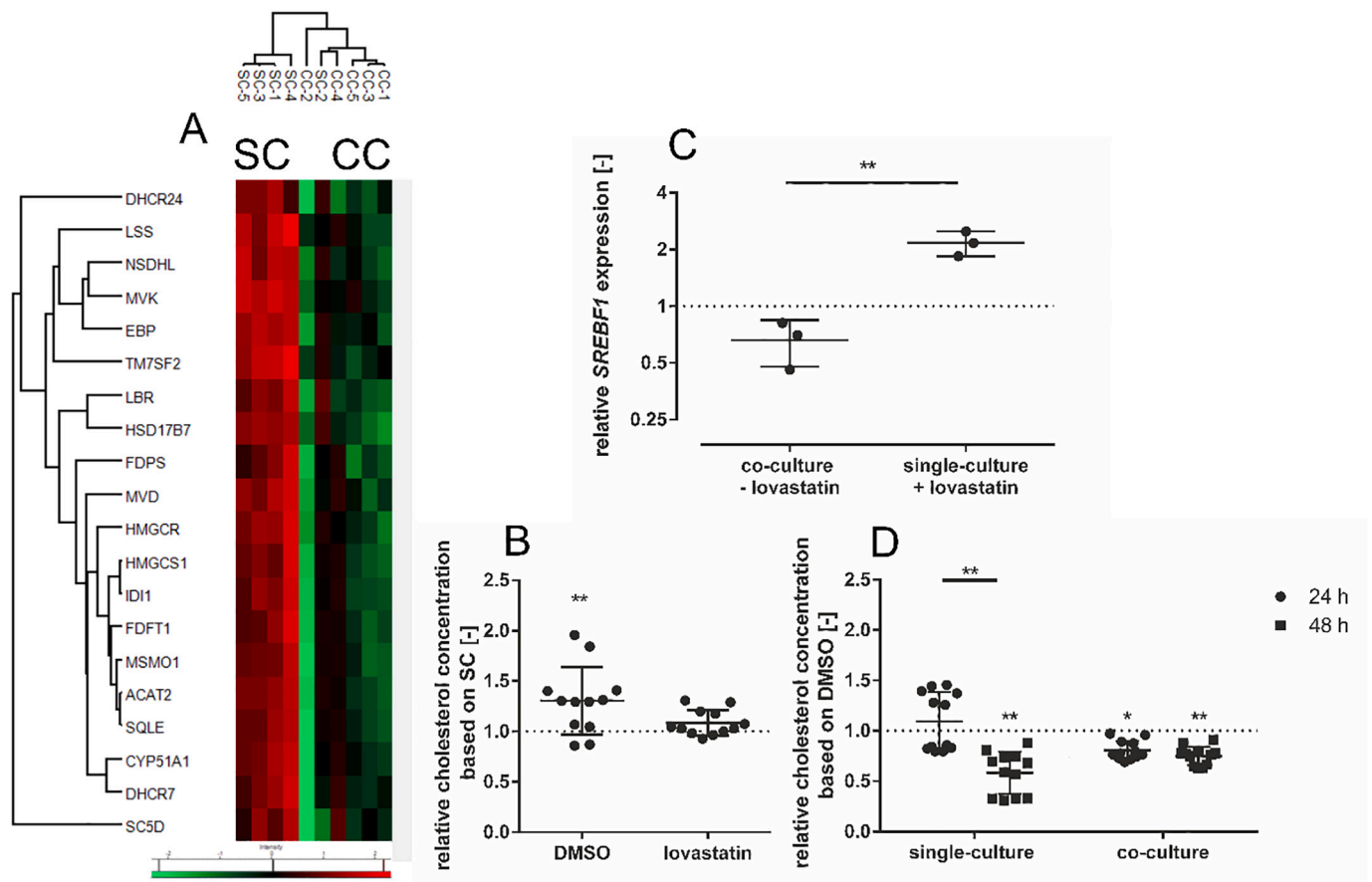
Fig. 6. Effects of co-culture on cholesterol biosynthesis. (A) Heat map of HepG2 cells in single culture (SC) or HepG2 cells co-cultured (CC) with PMA-differentiated THP-1 cells after 24 h ($n = 5$). The gene symbols and the Z-score of significantly (exclusion $p > 0.05$) expressed genes are shown. (B) Co-cultivation increased the relative cholesterol concentration in co-cultivated HepG2 cells. This increase was suppressed by 1 μM lovastatin. (C) Lovastatin (1 μM) increased the expression of sterol regulatory element binding transcription factor 1 (*SREBF1*) in individually cultivated HepG2 cells. During co-cultivation, the expression of SREBF1 was decreased in HepG2 cells ($n = 3$). (D) Cholesterol concentration in co-cultivated lovastatin-treated HepG2 cells decreased after 24 h and remained constant for 48 h. Cholesterol concentration in individually cultivated HepG2 cells decreased after 48 h relative to the corresponding DMSO control. Measurement data (•,■), mean ± SD and respective control (⋯) are shown. *$p < 0.05$ and **$p < 0.01$.

genes related to lipid metabolism were upregulated in co-culture (Fig. 7A). However, these significantly upregulated genes could not be assigned to a distinct lipid metabolic pathway. Therefore, we quantified the amount of lipid droplets in HepG2 cells upon individual cultivation and co-cultivation. In general, the total area of lipid droplets in HepG2 cells was significantly ($p < 0.01$) reduced in co-culture by 76% (Fig. 7B). To further elucidate this result, we studied the expression and concentration of fatty acid synthase (FAS), a key enzyme in lipid synthesis. The gene array data (Fig. 7A) and qPCR showed that the expression of *FASN* in HepG2 cells was significantly downregulated by 0.6-fold and that the protein concentration was reduced by 0.7-fold under co-culture conditions, supporting the reduction in the amount of lipid droplets (Fig. 7C + D).

Accordingly, total lipid synthesis seems to be lowered in co-cultivated HepG2 cells.

3.7. Co-culture activates key events of the AOP fibrosis

The global transcriptome analysis of the co-culture indicated an increased expression of genes related to liver fibrosis. To validate this prediction, we studied key events (KE) of the adverse outcome pathway number 38 (Landesmann, 2016), visualized the presence of extracellular collagen and determined the upregulation of fibrosis-related

genes (Fig. 8). The 'KE 1' requires hepatocyte injury. Hepatocyte injury is often related to the amount of intracellular ATP, which was significantly ($p < 0.01$) reduced in co-cultivated HepG2 cells (Fig. 8B). 'KE 2' is the activation of Kupffer cells (KC). The transcriptome analysis of all associated genes (*e.g.*, cytokines and corresponding receptors) showed KC activation. In brief, 86% of all significantly ($p < 0.05$) regulated genes examined for KE 2 were upregulated (Fig. 8C). Regarding 'KE 3', enhanced *TGFB1* expression was detected (up to 1.7-fold) in co-cultivated HepG2 cells compared to individually cultivated cells (Fig. 8D). The activation of these key events should result in an accumulation of collagen in the co-culture system. Staining and photometric quantification shows that a rather small but significant ($p < 0.05$) accumulation (1.14-fold) of collagen occurred in co-cultivated HepG2 cells (Fig. 8E). In order to validate these unexpected finding further, the presence of extracellular collagen was analysed using Sirius Red (Fig. 8F). The images clearly proved, that staining occurred in cells and not, as expected for the extracellular matrix, outside of the cells. Finally, the expression of genes related to fibrosis was studied. In the co-culture the expression of pro-fibrotic genes for smooth muscle α actin (*ACTA2*) and SMAD family member 7 (*SMAD7*) were down-regulated and only the expression of SMAD family member 3 (*SMAD3*) was upregulated, relative to the single cultured HepG2 cells (Fig. 8G).
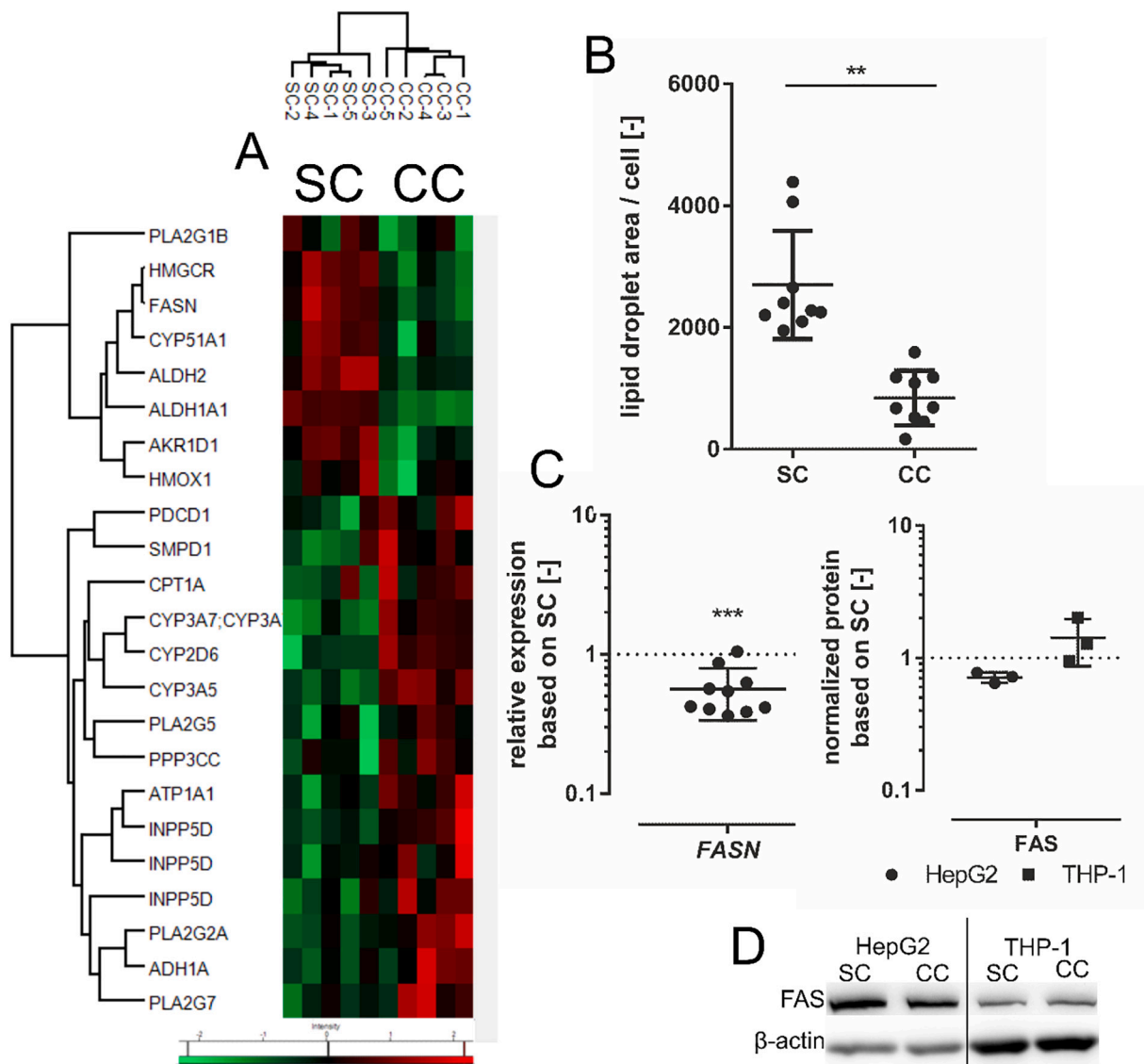
Fig. 7. Lipid metabolism. (A) Heat map of differentially expressed genes in HepG2 cells in single culture (SC) and co-culture (CC) with PMA-differentiated THP-1 cells. The gene symbols and the *Z*-score (exclusion $p > 0.05$) after 24 h are shown ($n = 5$). (B) Effect of SC and CC on the intracellular lipid droplet area (normalized to cell number) of HepG2 cells after 24 h ($n = 3$). Each dot (●) represents a microscopic image. (C) HepG2 cells cultivated for 24 h in CC, showed reduced expression of fatty acid synthase (*FASN*) normalized to SC (···) and HPRT ($n = 10$). The amount of fatty acid synthase (FAS) protein in CC was slightly reduced compared to in the SC (···) of HepG2 (●) or THP-1 (■) cells ($n = 3$). (D) Amount of FAS protein under SC and CC conditions. $**p < 0.01$, $***p < 0.005$.

In summary, while several of the KEs of the AOP fibrosis are met, the co-culture does not represent a fibrotic state and is in its present form not useful for studying fibrosis.

4. Discussion

In this study, we characterized changes at the cellular level that were induced by the co-cultivation of HepG2 and PMA-differentiated THP-1 cells. The main focus was on the hepatic cell line. Transcriptome analyses of co-cultivated and individually cultivated HepG2 cells were taken as the basis for all further investigations. The previously reported pro-inflammatory properties of this co-culture (Wewering et al., 2017a; Granitzny et al., 2017; Wewering et al., 2017b) were studied in close detail in order to characterize the system further. Except for IL-1α, the concentrations of all detected cytokines were found increased in the supernatant of co-cultivated cells (Fig. 4B).

Next, we compared the cytokine concentration measured under co-cultivation conditions with reported serum concentrations of healthy humans. The IL-6 concentration in our *in vitro* model was in a similar

range as found in healthy human serum (Table 1), and GM-CSF is the only cytokine that showed a lower concentration than the reported values (Table 1). All other detected cytokines (IL-8, TGF-α, G-CSF, TGF-β, hFGF) had higher concentrations in the supernatant of the co-culture than in healthy human serum (Table 1). Even though that the absolute numbers of the *in vitro* concentrations are not directly comparable with the *in vivo* data, the concentrations are in the same range. Surprisingly, IL-1α was only detected in the supernatant of THP-1 cells under single culture conditions (Fig. 4B). Under co-cultivation conditions, no secretion was detectable, hence indicating that indirect cell-cell interactions (HepG2-THP-1) occurred. Therefore, co-cultivation is associated with the release of the inflammatory cytokines IL-8, TGF-α and G-CSF in the supernatant, most likely due to complex cell-cell interactions.

Xenobiotic metabolism is also affected in a pro-inflammatory environment. An increase in the IL-6 serum levels of patients undergoing allogeneic bone marrow transplantation was associated with a decrease in cyclosporine metabolism (Chen et al., 1994). The liver is important for phase I and phase II metabolism of xenobiotic substances (Anzenbacher and Zanger, 2012), and it has been shown that cytokines
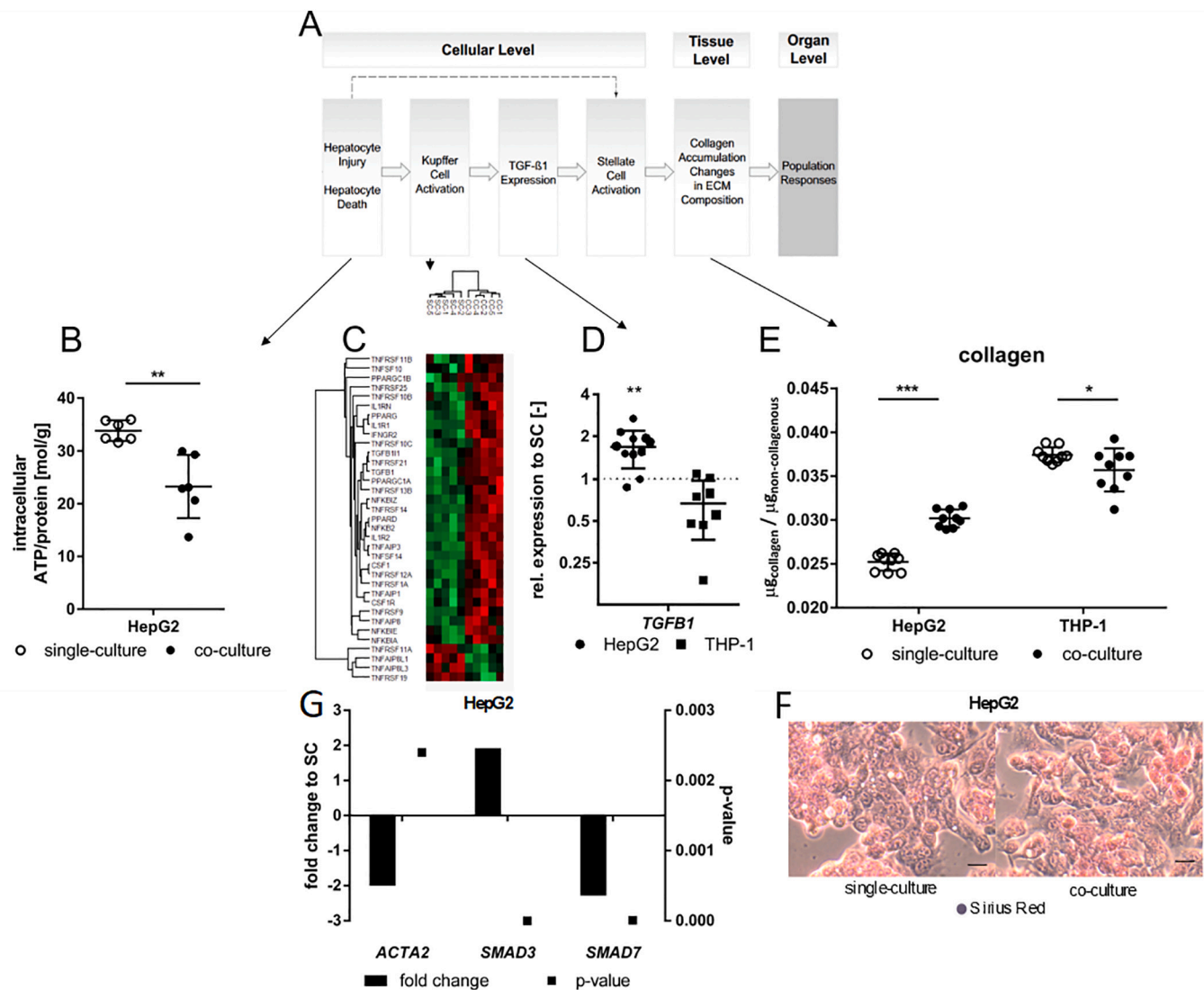
Fig. 8. Application of key events of the adverse outcome pathway (AOP) of 'fibrosis' (A) AOP analysis according to Horvat and co-workers (Horvat et al., 2017), including the gene symbol of transforming growth factor β 1 (*TGFB1*) and the extracellular matrix (ECM). (B) ATP concentration per g total protein of HepG2 cells cultivated for 24 h under single culture (SC) or co-culture conditions (CC) with PMA-differentiated THP-1 cells. Individual measurement data (○, ●), mean ± SD are given (*n* = 3). (C) HepG2 cells were cultivated under SC or CC for 24 h (*n* = 5). The gene symbols and the *Z*-score of significantly (exclusion *p* > 0.05) and differentially expressed relevant genes for Kupffer cell activation are shown (Horvat et al., 2017). An enlarged heat map is shown in supplementary fig. S3. (D) Expression of *TGFB1* normalized to SC (⋯) HepG2 cells or PMA-differentiated THP-1 cells (■) and HPRT are shown (*n* = 11). (E) The concentration of collagen significantly increased under the CC with HepG2 cells and PMA-differentiated THP-1 within 24 h. Data were normalized to the total amount of non-collagenous protein (n = 3). (F) Representative microscopic image of HepG2 cells after cultivation under SC or CC for 24 h. The collagen staining (Sirius Red) was exclusively detectable in the intracellular compartments. (G) Fold change (CC relative to SC, n = 5) of fibrosis associated gene expression assessed from the transcriptomic analysis, including the respective *p*-value. The gene for smooth muscle α actin (*ACTA2*) and SMAD family member 7 (*SMAD7*) were downregulated in CC compared to SC, while SMAD family member 3 (*SMAD3*) was upregulated. *$p < 0.05$, **$p < 0.01$, and ***$p < 0.005$. (For interpretation of the references to colour in this figure legend, the reader is referred to the web version of this article.)

can affect biotransformation (Prescott et al., 1975). Xenobiotic metabolism (membrane transport, phase I and phase II) is reduced by 10 ng/ml IL-6 in primary human hepatocytes and HepaRG cells (Klein et al., 2015). In addition, the phase I enzyme CYP1A1 is repressed by IL-6 and TNF-α in primary human hepatocytes (Muntane-Relat et al., 1995). Previously, we have shown that the secretion of TNF-α increases under co-cultivation conditions up to 63.5 pg/ml (Padberg et al., 2019), and here we report that the IL-6 concentration was 3.9 pg/ml (Table 1). In contrast to the reported data (Muntane-Relat et al., 1995), CYP1A1 enzyme activity also increased (Fig. 5E), indicating that the interaction of cytokines and xenobiotic metabolism might be more complex and different in the HepG2 and THP-1 co-culture system than in individually cultivated primary hepatocytes. The upregulation of CYP1A1

in the co-cultivated HepG2 cells could also be induced by other non-investigated pathways/receptors, such as the constitutive androstane receptor (CAR) and the liver X receptor α signalling (LXRα) pathways (Santes-Palacios et al., 2016). Indeed, the AHR pathway was activated in co-cultivated HepG2 cells. An assessment based on the higher concentration of AHR (Fig. 5B) and upregulated expression of the target genes *CYP1A1*, *CPY1A2* and *CYP1B1* (Fig. 5C). Interestingly, Nguyen and co-workers showed that humans exposed to dioxin (a potent activator of the AHR pathway) showed significantly increased gene expression of *TNF* and *IL-6* in whole blood cells (Nguyen et al., 2017). In addition to ligand-dependent activation, AHR overexpression can also result from the expression of IL-6 (Chen et al., 2011). Therefore, we concluded that the expression and activation of AHR in the co-culture

Table 1

Comparison of cytokine concentration in the supernatant of co-cultivated HepG2 cells with THP-1 cells and healthy human serum. The following cytokines were quantified: interleukin 8 (IL-8), transforming growth factor α (TGF-α), interleukin 6 (IL-6), granulocyte macrophage colony-stimulating factor (GM-CSF), granulocyte colony stimulating factor (G-CSF), transforming growth factor β (TGF-β), human fibroblast growth factor (hFGF) and interleukin 1 α (IL-1α). The mean concentration (± SD) in the co-culture supernatant and the mean concentration and concentration range in human serum are shown.

Cytokine	Concentration in co-culture [pg/ml] (SD)	Mean concentration (range) in healthy human serum [pg/ml]	Reference for serum concentrations
IL-8	> 12,603.06 (−)	29.3 (24.4–35.9)	(Kleiner et al., 2013)
TGF-α	56.87 (27.47)	3.2 (0.93–26.8)	(Kim et al., 2011)
IL-6	3.95 (0.58)	2.91 (0.16–37.7)	(Kim et al., 2011)
GM-CSF	10.22 (3.33)	38.3 (26.3–63.8)	(Kleiner et al., 2013)
G-CSF	1162.29 (485.3)	45.5 (34–53.6)	(Kleiner et al., 2013)
TGF-β	96.37 (90.08)	49.1 (not given)	(Wu et al., 2002)
hFGF	138.48 (110.09)	41.7 (33.2–49.5)	(Kleiner et al., 2013)
IL-1α	< 1.89	< 1.4	(Kleiner et al., 2013)

resulted from increased cytokine signalling, which finally results in an increased enzyme activity (Fig. 5E).

In addition to the biotransformation of xenobiotics, the liver is crucial for lipid metabolism, including cholesterol biosynthesis (Repa and Mangelsdorf, 2000). The biosynthesis of cholesterol increases in the co-culture system (Fig. 6), while the amount of total lipids, determined as lipid droplets, is reduced (Fig. 7B).

An increase in the sensitivity of co-cultured HepG2 cells towards lovastatin, a classical sterol biosynthesis inhibitor, occurred under co-cultivation (Fig. 6D). Lovastatin (HMG-CoA reductase inhibitor) reduced the cholesterol concentration in the co-culture after 24 h. In contrast, the reduction occurred in single-cultivated HepG2 only after 48 h. This result demonstrates that the co-culture system has an improved sensitivity towards a classical sterol biosynthesis inhibitor. Previously, enhanced sensitivity to the DILI-inducing substance ketoconazole was demonstrated due to increases in oxidative stress-related proteins and pro-inflammatory cytokine secretion (Wewering et al., 2017a). This finding was supported by a mechanistic approach, testing a larger set of drugs (Granitzny et al., 2017). Therefore, it is concluded that the co-culture exhibits not only a higher sensitivity to DILI-inducing substances but might also respond more rapidly to drug exposure. This has to be studied in more detail in future. Whether this enhanced sensitivity is based on the reduced lipid droplets in the co-cultivated HepG2 (Fig. 7B) remains also to be proven. It is known that lipid droplets maintain organelle homeostasis and prevent reactive oxygen species (ROS), lipid overload, hypoxia and apoptotic cell death (Baenke et al., 2013).

Surprisingly, the increased cholesterol biosynthesis (Fig. 6) does not lead to an increase in total lipids (Fig. 7B), but rather to a decrease in the number of lipid droplets. Since acetyl-CoA is the common precursor of cholesterol and fatty acids, it can be concluded that acetyl-CoA is not limited and that the regulation of the two pathways must occur at later stages. We identified a decrease in the lipid droplet area per cell (Fig. 7B) and validated the hypothesis that de novo fatty acid (FA) synthesis was reduced in co-culture, since the gene expression of FAS and the amount of FAS protein was decreased in the co-culture compared to the individual cultures (Fig. 7C + D). The reduction of FAS and the lipids indicates, that the β-oxidation of FA is increased in co-cultivation compared to HepG2 cells alone, thereby providing ATP. The decreased intracellular ATP amount in co-cultivated HepG2 cells supports this (Fig. 8B). An increased CYP expression (Fig. 5C) and protein biosynthesis (Fig. 5E) supports the need for energy further, because protein biosynthesis is one of the most energy consuming cellular processes (Lindqvist et al., 2018). Also the enhanced cholesterol biosynthesis in co-cultivation (Fig. 6) is an ATP demanding anabolic

pathway (Korman et al., 2014). Taken together the co-cultivated HepG2 cells have an higher ATP demand compared to the HepG2 cells alone and this is most likely covered by the oxidation of FA.

The aforementioned changes in lipid metabolism can be closely linked to the inflammatory environment during co-cultivation. The hormone leptin promotes FA oxidation, resulting in a reduction of hepatic triglycerides and cytokine secretion (GM-CSF, IL-1α, IL-1β, IL-6, IL-10 and IL-18) in murine KC *in vitro* (Metlakunta et al., 2017). However, the authors showed that typical leptin-induced FA oxidation was not a consequence of the cytokine release (Metlakunta et al., 2017). This result provides evidence that the interplay of the cytokines with each other and with cells and tissues is complex. IL-6 is a pleiotropic cytokine and has multiple effects on hepatic lipid metabolism (Hassan et al., 2014). In general, lipid metabolism is disturbed during inflammatory processes (Tall and Yvan-Charvet, 2015).

The inflammatory pattern of the co-culture does not indicate a pathophysiological pattern like non-alcoholic fatty liver disease (NAFLD) or steatohepatitis, even though the typical pro-inflammatory cytokines (*e.g.*, IL-6, IL-8 and TNF-α) are increased (Braunersreuther et al., 2012; Niederreiter and Tilg, 2018). Since the lipid droplet area in the presented co-culture was reduced (Fig. 7B), the system did not represent a true model of fatty liver disease.

A pro-inflammatory co-culture system might also enable the investigation of liver fibrosis *in vitro*. Liver fibrosis is associated with abundant extracellular matrix (ECM) proteins, like collagen. Hepatic stellate cells are the main mediators of ECM production (Bataller and Brenner, 2005). Recently, Prestigiacomo and co-workers (Prestigiacomo et al., 2017) developed a co-culture system, composed of three cell lines: HepaRG, differentiated THP-1 and hTERT-HSC for studying fibrosis. ECM production and fibrosis become clinically relevant when dysregulated, eventually leading to chronic liver diseases (Pellicoro et al., 2014). This liver injury can be induced *in vitro* using the indirect co-cultivation of rat hepatic stellate cells and rat KCs (Nieto, 2006). In the presented co-cultivation system, the main key events of the AOP for fibrosis (Horvat et al., 2017) were observable (Fig. 8). Due to the absence of stellate cells, however, we were unable to prove key event 4, that is, the activation of the latter cell type. Stellate cells are an essential contributor to hepatic fibrosis (Horvat et al., 2017). A small but significant collagen accumulation, could be confirmed (Fig. 8E) in HepG2 cells. The synthesis of collagen 1 by HepG2 cells has been reported (Zhang et al., 2020), and that collagen production can be induced by 10 μM all-*trans* retinoic acid (Wang et al., 2013). This finding shows that stellate cell-independent collagen accumulation can occur *in vitro*. While several KE of the AOP fibrosis were detected in our co-culture system, it does not represent a fibrotic state, because there was no extracellular accumulation of collagen (Fig. 8F). In addition, *ACTA2* and *SMAD7* (Rockey et al., 2019), important during the development of fibrosis were downregulated (Fig. 8G) and only *SMAD3* was upregulated, relative to the single culture. Therefore, this example demonstrates, that AOPs should be used with care. The presence of KE are important parameters in an AOP, but in the case of complex pathological processes like fibrosis the presence of KE might be misleading. Especially, if *in vitro* systems do not consist of the cell types relevant for the pathological process. Stellate cells in the case of fibrosis. This is clearly demonstrated by an *in vitro* co-culture system of HepRG, THP-1 and a stellate cell line, that is able to mimic the fibrotic pathology (Prestigiacomo et al., 2017).

5. Conclusion

Biochemical changes that were induced by the co-cultivation of HepG2 and PMA-differentiated THP-1 cells were characterized. In general, indirect co-cultivation was associated with an inflammatory cytokine composition in the supernatant. Enzymes involved in xenobiotic metabolism (CYP1A1, CYP1A2 and CYP1B1) increased, as determined by mRNA expression. Besides differential gene expression the

enzymatic activity also increased. These observations were due to activation of the AHR signalling pathway. In addition, the lipid metabolism was disturbed, indicated by an increased cholesterol biosynthesis, a shortened reaction time upon lovastatin treatment, and a reduced *de novo* fatty acid synthesis.

In summary, the co-culture of HepG2 and PMA-differentiated THP-1 is a simple *in vitro* method with increased release of inflammatory cytokines (IL-8, TGF-β, IL-6, GM-CSF, G-CSF, TGF-β and hFGF) and an activated AHR pathway with differential expression of genes related to biotransformation and an increased CYP1A1 enzymatic activity. Finally, we consider that this co-cultivation is a method for a fast and uncomplicated screening of substances that affect the release of pro-inflammatory cytokines or AHR signalling and related enzyme activities.

Declaration of Competing Interest

The authors declare that they have no known competing financial interests or personal relationships that could have appeared to influence the work reported in this paper.

Acknowledgements

Appendix A. Supplementary data

Supplementary data to this article can be found online at https://doi.org/10.1016/j.tiv.2020.104957.

References

Albrecht, W., Kappenberg, F., Brecklinghaus, T., Stoeber, R., Marchan, R., Zhang, M., Ebbert, K., Kirschner, H., Grinberg, M., Leist, M., Moritz, W., Cadenas, C., Ghallab, A., Reinders, J., Vartak, N., van Thriel, C., Golka, K., Tolosa, L., Castell, J.V., Damm, G., Seehofer, D., Lampen, A., Braeuning, A., Buhrke, T., Behr, A.-C., Oberemm, A., Gu, X., Kittana, N., van de Water, B., Kreiling, R., Fayyaz, S., van Aerts, L., Smedsrød, B., Ellinger-Ziegelbauer, H., Steger-Hartmann, T., Gundert-Remy, U., Zeigerer, A., Ullrich, A., Runge, D., Lee, S.M.L., Schiergens, T.S., Kuepfer, L., Aguayo-Orozco, A., Sachinidis, A., Edlund, K., Gardner, I., Rahnenführer, J., Hengstler, J.G., 2019. Prediction of human drug-induced liver injury (DILI) in relation to oral doses and blood concentrations. Arch. Toxicol. 93 (6), 1609–1637.
Anzenbacher, P., Zanger, U.M., 2012. Metabolism of Drugs and Other Xenobiotics. Wiley-VCH, Weinheim.
Baenke, F., Peck, B., Miess, H., Schulze, A., 2013. Hooked on fat: the role of lipid synthesis in cancer metabolism and tumour development. Dis. Model. Mech. 6 (6), 1353–1363.
Bataller, R., Brenner, D.A., 2005. Liver fibrosis. J. Clin. Invest. 115 (2), 209–218.
Braunersreuther, V., Viviani, G.L., Mach, F., Montecucco, F., 2012. Role of cytokines and chemokines in non-alcoholic fatty liver disease. World J. Gastroenterol. 18 (8), 727–735.
Bro, R., Smilde, A.K., 2014. Principal component analysis. Anal. Methods 6 (9), 2812–2831.
Carpenter, A.E., Jones, T.R., Lamprecht, M.R., Clarke, C., Kang, I.H., Friman, O., Guertin, D.A., Chang, J.H., Lindquist, R.A., Moffat, J., Golland, P., Sabatini, D.M., 2006. CellProfiler: image analysis software for identifying and quantifying cell phenotypes. Genome Biol. 7 (10), R100.
Chen, Y.L., Le Vraux, V., Leneveu, A., Dreyfus, F., Stheneur, A., Florentin, I., De Sousa, M., Giroud, J.P., Flouvat, B., Chauvelot-Moachon, L., 1994. Acute-phase response, interleukin-6, and alteration of cyclosporine pharmacokinetics. Clin. Pharmacol. Ther. 55 (6), 649–660.
Chen, P.H., Chang, H., Chang, J.T., Lin, P., 2011. Aryl hydrocarbon receptor in association with RelA modulates IL-6 expression in non-smoking lung cancer. Oncogene 31, 2555.
Granitzny, A., Knebel, J., Muller, M., Braun, A., Steinberg, P., Dasenbrock, C., Hansen, T., 2017. Evaluation of a human in vitro hepatocyte-NPC co-culture model for the prediction of idiosyncratic drug-induced liver injury: a pilot study. Toxicol. Rep. 4, 89–103.
Hassan, W., Ding, L., Gao, R.Y., Liu, J., Shang, J., 2014. Interleukin-6 signal transduction and its role in hepatic lipid metabolic disorders. Cytokine 66 (2), 133–142.
Hewitt, N.J., Hewitt, P., 2004. Phase I and II enzyme characterization of two sources of HepG2 cell lines. Xenobiotica 34 (3), 243–256.
Horvat, T., Landesmann, B., Lostia, A., Vinken, M., Munn, S., Whelan, M., 2017. Adverse outcome pathway development from protein alkylation to liver fibrosis. Arch.

Toxicol. 91 (4), 1523–1543.
Kim, H.O., Kim, H.S., Youn, J.C., Shin, E.C., Park, S., 2011. Serum cytokine profiles in healthy young and elderly population assessed using multiplexed bead-based immunoassays. J. Transl. Med. 9, 113.
Klein, M., Thomas, M., Hofmann, U., Seehofer, D., Damm, G., Zanger, U.M., 2015. A systematic comparison of the impact of inflammatory Signaling on absorption, distribution, metabolism, and excretion gene expression and activity in primary human hepatocytes and HepaRG cells. Drug Metab. Dispos. 43 (2), 273.
Kleiner, G., Marcuzzi, A., Zanin, V., Monasta, L., Zauli, G., 2013. Cytokine levels in the serum of healthy subjects. Mediat. Inflamm. 2013, 434010.
Korman, T.P., Sahachartsiri, B., Li, D., Vinokur, J.M., Eisenberg, D., Bowie, J.U., 2014. A synthetic biochemistry system for the in vitro production of isoprene from glycolysis intermediates. Protein Sci. 23 (5), 576–585.
Kurynina, A.V., Erokhina, M.V., Makarevich, O.A., Sysoeva, V.Y., Lepekha, L.N., Kuznetsov, S.A., Onishchenko, G.E., 2018. Plasticity of human THP–1 cell phagocytic activity during Macrophagic differentiation. Biochem. Mosc. 83 (3), 200–214.
Landesmann, B., 2016. Adverse Outcome Pathway on Protein Alkylation Leading to Liver Fibrosis. OECD Publishing OECD Series on Adverse Outcome Pathways, No. 2.
Lin, J., Schyschka, L., Muhl-Benninghaus, R., Neumann, J., Hao, L., Nussler, N., Dooley, S., Liu, L., Stockle, U., Nussler, A.K., Ehnert, S., 2012. Comparative analysis of phase I and II enzyme activities in 5 hepatic cell lines identifies Huh-7 and HCC-T cells with the highest potential to study drug metabolism. Arch. Toxicol. 86 (1), 87–95.
Lindqvist, L.M., Tandoc, K., Topisirovic, I., Furic, L., 2018. Cross-talk between protein synthesis, energy metabolism and autophagy in cancer. Curr. Opin. Genet. Dev. 48, 104–111.
Livak, K.J., Schmittgen, T.D., 2001. Analysis of relative gene expression data using real-time quantitative PCR and the 2(T)(− Delta Delta C) method. Methods 25 (4), 402–408.
Lund, M.E., J. To, O'Brien, B.A., Donnelly, S., 2016. The choice of phorbol 12-myristate 13-acetate differentiation protocol influences the response of THP-1 macrophages to a pro-inflammatory stimulus. J. Immunol. Methods 430, 64–70.
Metlakunta, A., Huang, W., Stefanovic-Racic, M., Dedousis, N., Sipula, I., O'Doherty, R.M., 2017. Kupffer cells facilitate the acute effects of leptin on hepatic lipid metabolism. Am. J. Physiol. Endocrinol. Metab. 312 (1), E11–E18.
Mosmann, T., 1983. Rapid colorimetric assay for cellular growth and survival: application to proliferation and cytotoxicity assays. J. Immunol. Methods 65 (1–2), 55–63.
Muntane-Relat, J., Ourlin, J.C., Domergue, J., Maurel, P., 1995. Differential effects of cytokines on the inducible expression of CYP1A1, CYP1A2, and CYP3A4 in human hepatocytes in primary culture. Hepatology 22 (4), 1143–1153 Pt 1.
Nguyen, C.H., Nakahama, T., Dang, T.T., Chu, H.H., Van Hoang, L., Kishimoto, T., Nguyen, N.T., 2017. Expression of aryl hydrocarbon receptor, inflammatory cytokines, and incidence of rheumatoid arthritis in Vietnamese dioxin-exposed people. J. Immunotoxicol. 14 (1), 196–203.
Niederreiter, L., Tilg, H., 2018. Cytokines and fatty liver diseases. Liver Research 2 (1), 14–20.
Nieto, N., 2006. Oxidative-stress and IL-6 mediate the fibrogenic effects of [corrected] Kupffer cells on stellate cells. Hepatology 44 (6), 1487–1501.
Padberg, F., Tarnow, P., Luch, A., Zellmer, S., 2019. Minor structural modifications of bisphenol a strongly affect physiological responses of HepG2 cells. Arch. Toxicol. 93 (6), 1529–1541.
Pellicoro, A., Ramachandran, P., Iredale, J.P., Fallowfield, J.A., 2014. Liver fibrosis and repair: immune regulation of wound healing in a solid organ. Nat. Rev. Immunol. 14, 181.
Plotly Technologies Inc, 2015. Collaborative Data Science, Plotly Technologies Inc., Montréal. https://plot.ly/create/.
Prescott, L.F., Forrest, J.A., Adjepon-Yamoah, K.K., Finlayson, N.D., 1975. Drug metabolism in liver disease. J. Clin. Pathol. Suppl. (R. Coll. Pathol.) 9, 62–65.
Prestigiacomo, V., Weston, A., Messner, S., Lampart, F., Suter-Dick, L., 2017. Pro-fibrotic compounds induce stellate cell activation, ECM-remodelling and Nrf2 activation in a human 3D-multicellular model of liver fibrosis. PLoS One 12 (6), e0179995.
Repa, J.J., Mangelsdorf, D.J., 2000. The role of orphan nuclear receptors in the regulation of cholesterol homeostasis. Annu. Rev. Cell Dev. Biol. 16, 459–481.
Rockey, D.C., Du, Q., Shi, Z., 2019. Smooth muscle α-actin deficiency leads to decreased liver fibrosis via impaired cytoskeletal Signaling in hepatic stellate cells. Am. J. Pathol. 189 (11), 2209–2220.
Roth, R.A., Luyendyk, J.P., Maddox, J.F., Ganey, P.E., 2003. Inflammation and drug idiosyncrasy–is there a connection? J. Pharmacol. Exp. Ther. 307 (1), 1–8.
Santes-Palacios, R., Ornelas-Ayala, D., Cabanas, N., Marroquin-Perez, A., Hernandez-Magana, A., Del Rosario Olguin-Reyes, S., Camacho-Carranza, R., Espinosa-Aguirre, J.J., 2016. Regulation of human cytochrome P4501A1 (hCYP1A1): a plausible target for chemoprevention? Biomed. Res. Int. 2016, 5341081.
Schwende, H., Fitzke, E., Ambs, P., Dieter, P., 1996. Differences in the state of differentiation of THP-1 cells induced by phorbol ester and 1,25-dihydroxyvitamin D3. J. Leukoc. Biol. 59 (4), 555–561.
Shimano, H., Horton, J.D., Hammer, R.E., Shimomura, I., Brown, M.S., Goldstein, J.L., 1996. Overproduction of cholesterol and fatty acids causes massive liver enlargement in transgenic mice expressing truncated SREBP-1a. J. Clin. Invest. 98 (7), 1575–1584.
Soldatow, V.Y., Lecluyse, E.L., Griffith, L.G., Rusyn, I., 2013. In vitro models for liver toxicity testing. Toxicol Res (Camb) 2 (1), 23–39.
Tall, A.R., Yvan-Charvet, L., 2015. Cholesterol, inflammation and innate immunity. Nat. Rev. Immunol. 15, 104.
Toyoda, Y., Kashikura, K., Soga, T., Tagawa, Y.I., 2017. Metabolomics of an in vitro liver model containing primary hepatocytes assembling around an endothelial cell network: comparative study on the metabolic stability and the effect of acetaminophen treatment. J. Toxicol. Sci. 42 (4), 445–454.
Tyanova, S., Temu, T., Sinitcyn, P., Carlson, A., Hein, M.Y., Geiger, T., Mann, M., Cox, J.,

2016. The Perseus computational platform for comprehensive analysis of (prote) omics data. Nat. Methods 13, 731.

Wang, W., Xu, G., Ding, C.L., Zhao, L.J., Zhao, P., Ren, H., Qi, Z.T., 2013. All-trans retinoic acid protects hepatocellular carcinoma cells against serum-starvation-induced cell death by upregulating collagen 8A2. FEBS J. 280 (5), 1308–1319.

Wewering, F., Jouy, F., Wissenbach, D.K., Gebauer, S., Blüher, M., Gebhardt, R., Pirow, R., von Bergen, M., Kalkhof, S., Luch, A., Zellmer, S., 2017a. Characterization of chemical-induced sterile inflammation in vitro: application of the model compound ketoconazole in a human hepatic co-culture system. Arch. Toxicol. 91 (2), 799–810.

Wewering, F., Jouy, F., Caliskan, S., Kalkhof, S., von Bergen, M., Luch, A., Zellmer, S., 2017b. Hepatic co-cultures in vitro reveal suitable to detect Nrf2-mediated oxidative stress responses on the bladder carcinogen o-anisidine. Toxicol. in Vitro 40, 153–160.

Wu, H.S., Li, Y.F., Chou, C.I., Yuan, C.C., Hung, M.W., Tsai, L.C., 2002. The concentration of serum transforming growth factor beta-1 (TGF-beta1) is decreased in cervical carcinoma patients. Cancer Investig. 20 (1), 55–59.

Zeilinger, K., Freyer, N., Damm, G., Seehofer, D., Knospel, F., 2016. Cell sources for in vitro human liver cell culture models. Exp. Biol. Med. (Maywood) 241 (15), 1684–1698.

Zhang, Q., Chang, X., Wang, H., Liu, Y., Wang, X., Wu, M., Zhan, H., Li, S., Sun, Y., 2020. TGF-β1 mediated Smad signaling pathway and EMT in hepatic fibrosis induced by Nano NiO in vivo and in vitro. Environ. Toxicol. 35 (4), 419–429.

Zhou, Y., Shen, J.X., Lauschke, V.M., 2019. Comprehensive evaluation of Organotypic and microphysiological liver models for prediction of drug-induced liver injury. Front. Pharmacol. 10, 1093.